



The Effect of Location and Shape of Vortex Generators on Aerodynamic Characteristics of a NACA 4415 Airfoil

Khuder N. Abed^{1*}

Authors affiliations:

1*) Mechanical Eng. Dept.,
Diyala University – Baqubah
City, Diyala, Iraq
khuder973@gmail.com

Paper History:

Received: 24th May. 2023

Revised: 24th June 2023

Accepted: 29th Aug. 2023

Abstract

This study examines the flow behavior and lift coefficient variations of a NACA 4415 airfoil using different vortex generator configurations. Experimental investigations are conducted in a subsonic wind tunnel at a Reynolds number of 1.8×10^5 . The airfoil is tested with two types of vortex generators, namely the dome vortex and the convergent-divergent vortex, positioned at 10%, 28%, and 60% chord locations. Experimental lift coefficients are compared with Airfoil Tools database, showing consistent agreement within an angle of attack range of 0 to 18 degrees. At small angles of attack (0 to 8 degrees), the lift coefficients of the NACA 4415 airfoil with the dome vortex at 10%, 28%, and 60% chord positions are lower compared to the baseline configuration. However, beyond 14 degrees, the highest lift coefficient value after the angle range of 14-18 degrees is achieved at the 60% chord position with the dome vortex, 10.43% increase compared to the baseline lift coefficient. Furthermore, the best value for the lift coefficient after the angle range of 16-18 degrees at the 10% chord position is achieved with the dome vortex, where the maximum lift coefficient 9.4% increase compared to the baseline lift coefficient. It is noted that the baseline configuration consistently outperforms the convergent-divergent vortex configurations.

Keywords: Aerodynamic Characteristics, NACA 4415 Airfoil, Vortex Generators, Lift Coefficient.

تأثير موقع وشكل مولدات الدوامات على الخصائص الديناميكية الهوائية لجهاز

NACA 4415 Airfoil

خضر نجم عبد

الخلاصة:

تبحث هذه الدراسة في سلوك التدفق واختلافات معامل الرفع لجناح NACA 4415 باستخدام تكوينات مختلفة لمولد الدوامة. يتم إجراء التحقيقات التجريبية في نفق رياح دون سرعة الصوت عند رقم رينولدز 1.8×10^5 . ويتم اختبار الجناح باستخدام نوعين من مولدات الدوامات، وهما دوامة القبة والدوامة المتقاربة المتباعدة، والمركزة عند 10% و 28% و 60%. تتم مقارنة معاملات الرفع التجريبية بالبيانات Airfoil Tools database، مما يُظهر تطابق متقارب ضمن زوايا الهجوم من 0 إلى 18 درجة. عند الزوايا الصغيرة للهجوم (من 0 إلى 8 درجات)، تكون معاملات الرفع لجناح NACA 4415 مع دوامة القبة عند 10% و 28% و 60% من مواضع الوتر أقل مقارنة بمعاملات رفع خط الأساس. ومع ذلك، بعد 14 درجات، يتم تحقيق أعلى قيمة لمعامل الرفع بعد نطاق الزاوية 14-18 درجة عند وضع الوتر 60% مع دوامة القبة، مما يؤدي إلى زيادة قدرها 10.43% مقارنة بمعامل الرفع الأساسي علاوة على ذلك، يتم تحقيق أفضل قيمة لمعامل الرفع بعد نطاق الزاوية 16-18 درجة عند موضع الوتر 10% مع دوامة القبة، حيث يتم تحقيق زيادة قدرها 9.4% في معامل الرفع مقارنة بالتكوين الأساسي. ويلاحظ أن التكوين الأساسي يتفوق باستمرار على تكوينات الدوامة المتقاربة والمتباعدة.

1. Introduction

Flow separation control has seen significant progress in refining high-lift device performance.

Active and passive flow control techniques, including vortex generators (VGs), play a crucial role in managing boundary and shear layer flows to



minimize separation over airfoils. Passive techniques alter the airfoil's shape and surface properties, while active techniques modify flow characteristics in real-time. The integration of these techniques is essential to overcome aerodynamic constraints and optimize performance. [1,2]. Hares et al. [3] conducted a comprehensive investigation into the effects of passive flow control using vortex generators (VGs) on the aerodynamic performance of the NACA 4415 airfoil. Through simulations and parameter exploration, the authors identified optimal VG dimensions and positions, resulting in improved lift coefficients, particularly at high angles of attack.

Fouatih et al. [4] performed wind tunnel experiments to optimize the NACA 4415 airfoil with VGs. By exploring different VG configurations, the study revealed a 21% increase in lift coefficient and a significant delay in flow separation. However, the introduction of micro VGs led to some increase in parasitic drag. Another study by Fouatih et al. [5] investigated the influence of passive VGs on the aerodynamic properties of the NACA 4415 airfoil using experimental and numerical approaches. The results demonstrated a strong agreement between experimental and computational findings, highlighting the optimized VG configuration that enhanced aerodynamic performance. Zulkefli, Nur Faraihan, et al. [6] focused on enhancing the lift-to-drag ratio of NACA 4415 airfoils using counter-rotating triangular or shark skin-shaped sub-boundary layer VGs. Wind tunnel tests revealed the superior performance of the shark skin-shaped VGs over triangular VGs, providing insights into innovative VG shapes for highly efficient airfoils. Muhammad et al. [7] investigated the effectiveness of hybrid micro VGs in controlling boundary layer separation in subsonic conditions. Their study demonstrated that hybrid micro VGs could significantly increase lift and improve the lift-to-drag ratio, offering a competitive alternative to traditional active VGs. Li, Xinkai, Ke Yang et al. [8] examined the impact of VG height on boundary layer control and aerodynamic performance using wind tunnel experiments and numerical methods. The study revealed a logarithmic relationship between VG height and vortex intensity, with significant improvements in maximum lift coefficient, stall angle, and drag coefficient. The study emphasized the importance of VG height in optimizing airfoil performance. Dadamoussa et al. [9] employed computational fluid dynamics simulations to investigate the performance enhancement of Darrieus wind turbines through a novel VG design. Their study demonstrated that selecting the appropriate VG size and position significantly improved the turbine's performance, particularly in terms of the tangential coefficient. Li, Xin-kai, et al. [10] examined the influence of VG spacing on flow control in wind turbine blades. Through numerical calculations and wind tunnel experiments, the study identified an optimal VG spacing that effectively suppressed boundary layer separation, improved lift-drag characteristics, and increased the stall angle of attack. Yan Yan et al. [11] conducted a numerical study on the aerodynamic performance of NACA

0018 airfoils and H-type Darrieus wind turbines with micro VGs. The optimized configuration of rectangular VGs significantly improved lift and stall angle for the airfoil. Additionally, the inclusion of VGs in the wind turbine enhanced power production and suppressed flow separation, demonstrating their potential impact on vertical axis wind turbine design.

Hao Chen [12] analyzed the influence of VG geometric parameters on the aerodynamic characteristics of the Bell A821201 airfoil. Computational fluid dynamics simulations revealed that VGs effectively delayed flow separation, resulting in increased lift, reduced drag, and improved aerodynamic performance. The paper by Li, Shuang, et al. [13] investigated the effects of VGs on the static and dynamic stall of the DU91-W2-250 wind turbine airfoil. Wind tunnel experiments were conducted to measure the impact of VGs on stall behavior. The results showed that VGs effectively controlled both static and dynamic stalls by creating lower pressure regions near the leading edge, delaying flow separation, and reducing pressure fluctuations during stall. Zhao, Zhenzhou, et al. [14] provided a comprehensive review of VGs' use to enhance wind turbine aerodynamic performance. The review covered the flow control principles of VGs and their validated ability to improve efficiency by delaying air separation on wind turbine blades. Hossain, Md Amzad, et al. [15] focused on the influence of dimple surface modifications on the aerodynamic characteristics of an airfoil. Their study demonstrated notable enhancements in lift force and stall angle of attack (AOA) with outward and inward dimples. Dimples effectively delayed flow separation and improved overall airfoil performance. Aftab, Syed Mohammed Aminuddin, et al. [16] explored the integration of tubercles on a NACA 4415 airfoil to improve lift and stall characteristics. The study revealed a significant 13.6% increase in lift with tubercles, surpassing conventional smooth wings and VGs. Tubercles also contributed to stall delay and sustained lift at high angles of attack. Arunvinthan, S., et al. [17] conducted wind tunnel tests on a NACA 0015 symmetrical airfoil incorporating shark scale-based vortex generators (SSVG). The SSVG integration resulted in reduced drag, increased maximum lift coefficient (CL_{max}), and improved overall aerodynamic performance. The study demonstrated the effectiveness of SSVG in inducing spanwise flow variation and positively influencing flow properties. Laffane, Zakarya, et al. [18] assessed the effectiveness of VGs on the aerodynamic performance of the NACA 63-215 airfoil. Their study revealed enhanced performance with a novel VG configuration, improving the maximum lift coefficient, reducing drag at high angles of attack, and increasing the lift-to-drag ratio. The study provided insights into the pressure distribution, velocity contours, and streamlines, illustrating how VGs enhance the airfoil's aerodynamic performance.

The aim of this research article is to conduct a comprehensive analysis of the impact of different vortex generator configurations on the lift coefficient of a NACA 4415 airfoil. The study aims to compare



the experimental lift coefficients with those obtained from a theoretical database, focusing on vortex generator positions at 10% chord, 28% chord, and 60% chord. The research investigates the influence of these vortex generator configurations on lift performance at various angles of attack. By examining the lift coefficient variations and comparing them to the baseline configuration, the study seeks to provide valuable insights into the aerodynamic behavior of the airfoil and determine the most effective vortex generator configuration for maximizing lift coefficients.

2. Methodology

2.1 Experimental Setup

The research examined the flow behavior over an airfoil of type NACA 4415 using two types of vortex generators at a Reynolds number of 1.8×10^5 . A locally constructed model has been developed to analyze the aerodynamics of the NACA 4415 airfoil. The data used for this particular section was sourced from NACA's lists of wings [20]. Furthermore, the wing section model features a chord length (C) of 18 cm and a span length (b) of 31.9 cm. During the study, a total of 20 pressure taps were strategically positioned on both the upper and lower surfaces of the wing. Two types of vortex generators were used. The first type is a dome vortex (DV), and the second type is a convergent-divergent vortex (CDV), both with dimensions as shown in Fig.1.

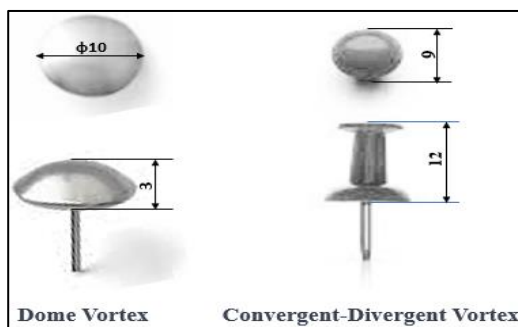


Figure (1): Dimensions and Types of Vortex Generators: Dome Vortex (DV) and Convergent-Divergent Vortex (CDV).

In this study, three sets of discrete vortex generators were used. The first set consisted of 15 vortex generators positioned 10% chord from the leading edge of the wing. This specific location was chosen because it is where the boundary layer is most prone to separating. The distance between the centers of the first and second vortex generators in this set was 10mm. The second set, also consisting of 15 vortex generators, was placed at a location on the upper surface of a NACA4415 airfoil that corresponds to 28% chord. This location was selected because it is where the boundary layer is most likely to transition into turbulence. Lastly, the third set, containing 15 vortex generators, was situated at a position on the wing's leading edge that corresponds to 60% chord. This placement was based on the understanding that the wing is more likely to experience separation due to an adverse

pressure gradient at this location. Refer to Figure 2 for a visual representation of these positions.

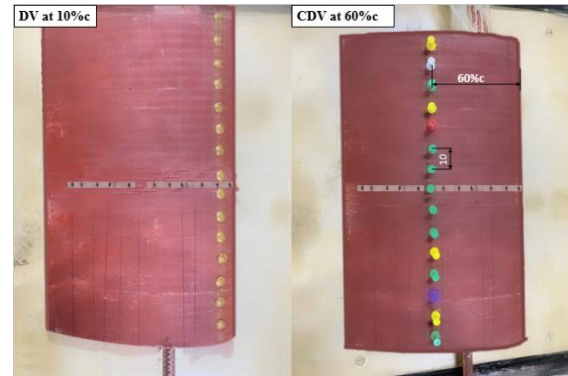


Figure (2): Distribution and Placement of Discrete Vortex Generators on a NACA4415 Airfoil

A NACA4415 airfoil placed inside an open-circuit subsonic wind tunnel. The wind tunnel has a working cross-section of 32cm x 32cm and was utilized to conduct experiments at ten different angles of attack ranging from 0° to 18° . The wind tunnel facility, located at the College of Engineering, University of Diyala, enabled the researchers to perform a comprehensive analysis of the incompressible air flow of subsonic aerodynamics with a satisfactory Reynolds number, given the maximum flow speed of 15 m/sec. The test section of the tunnel is fitted with a smooth contraction and a protective mesh screen to ensure flow uniformity.

2.2 Data Collection

To measure the surface pressure distribution, a standard multi-tube manometer consisting of 30 manometers was used. The manometer was connected to the stainless-steel pressure tubes over the wing section model via a rubber snout, as shown in Fig. 3. In this research, 11 pressure taps were used on the upper surface, and 9 taps were used on the lower surface of the wing, as previously shown in Fig. 2.



Figure (3): Setup of the Multi-tube Manometer for Measuring Surface Pressure Distribution

2.3 Data Analysis

To calculate the aerodynamic characteristics of the model from the pressure coefficient, aerodynamic pressure coefficients were subsequently calculated based on the pressure distribution over a NACA4415 model. The pressure distribution is represented in a dimensionless format utilizing the pressure coefficient (C_p) as described below [19]:

$$C_p = \frac{P_0 - P_\infty}{0.5\rho U_\infty^2} \quad \dots\dots (1)$$



In this equation, P_o denotes the surface pressure measured at a specific location on the surface, P_∞ represents the free stream pressure, ρ signifies air density, and U_∞ refers to the free-stream velocity, calculated using:

$$U_\infty = \sqrt{\frac{2(P_{stagnation} - P_\infty)}{\rho}} \quad \dots\dots (2)$$

Here, $P_{stagnation}$ is the stagnation pressure measured at the tip of the Pitot static tube. The vertical and axial force coefficients are obtained by integrating the pressure distribution along the chord, as demonstrated in the following equations:

$$C_x = \int_0^1 (C_{p_{lower}} - C_{p_{upper}}) \cdot d\left(\frac{x}{c}\right) \quad \dots\dots (3)$$

$$C_z = \int_{-z/c}^{z/c} (C_p) \cdot d\left(\frac{z}{c}\right) \quad \dots\dots (4)$$

Numerical solutions for eq. (3) and (4) are achieved using Simpson's numerical integration method, implementing 18 slices for both the upper and lower wing surfaces. The resulting lift and drag coefficients from pressure calculations are determined by these equations:

$$C_l = C_x \cos \alpha - C_z \sin \alpha \quad \dots\dots (5)$$

$$C_d = C_x \sin \alpha + C_z \cos \alpha \quad \dots\dots (6)$$

3. Results and discussions:

In this study, the measurements were conducted under specific atmospheric conditions, including a pressure of 1 atmosphere, a temperature of 20 degrees Celsius, a normal air density of 1.225 kg/m³, and a flow speed of 15 m/sec. The effects of two different vortex locations (dome vortex and converge-diverge vortex) on the lift coefficient of a NACA 4415 wing were discussed in this section. The drawbacks of vortex location were also discussed.

3.1 Effect of Vortex Location

Figure (4) presents a comprehensive comparison between the experimentally determined lift coefficient curve and the lift coefficient curve obtained from the Airfoil Tools database [20]. The analysis reveals a notable concurrence between the two curves, showing an increasing trend in the lift coefficient within the range of 0 to 18 degrees of angle of attack. However, beyond 18 degrees, a deviation occurs as the lift coefficient begins to decrease, indicating the onset of aerodynamic stall. Factors contributing to the differences between the practical and theoretical curves include the presence of surface roughness on the airfoil and suboptimal working conditions, such as variations in air density, temperature, and measurement tools. The experimental lift coefficient curve was considered the baseline for the current study, and all subsequent comparisons were made with it.

Figure (5) shows that at small angles of attack from 0 to 8, the lift coefficient values for the NACA 4415 wing with the dome vortex (DV) at 10% chord are lower than the baseline wing. This is due to unwanted airflow interference caused by the close

proximity of the vortex generator to the leading edge, resulting in flow distortions and improper aerodynamic separation [21]. As the angle increases beyond 8 degrees, the difference becomes smaller between the baseline lift coefficient and the lift coefficient with the dome vortex, but the baseline lift coefficient remains higher. Surprisingly, at 18 degrees, the lift coefficient with the dome vortex reaches its highest value of 1.27, surpassing the baseline value of 1.16. This represents a maximum lift coefficient increase of 9.4% compared to the baseline lift coefficient.

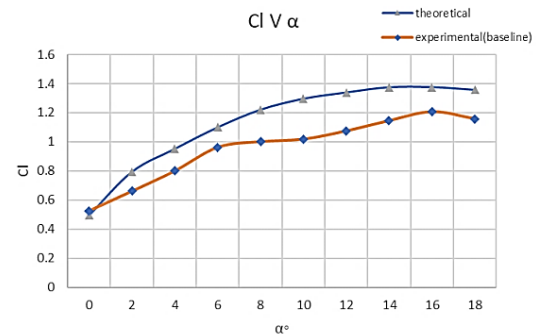


Figure (4): Comparative Analysis of Lift Coefficient Curves: Experimental vs. Airfoil Tools Database [20]

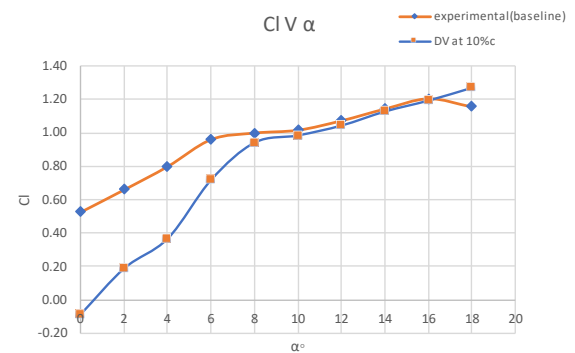


Figure (5): Effect of Dome Vortex at 10% Chord on Lift Coefficient for NACA 4415 Wing at Various Angles of Attack

Based on the data, Figure (6) show: At 0 degrees, baseline has C_l 0.52, slightly higher than dome vortex (0.44). With increasing angle of attack, both experience rising C_l , but dome vortex consistently has slightly lower values than baseline. At 8 degrees, dome vortex C_l 0.83 vs. baseline C_l 1, indicating slightly less lift. At 10 degrees, dome vortex C_l (1.00) closely matches baseline C_l (1.01), implying comparable lift. Generally, baseline exhibits higher lift, except for a few instances when dome vortex is comparable or slightly lower.

Figure (7) shows that when using the dome vortex configuration at 60% Chord, the lift coefficients increase, but they are still lower than the experimental baseline. The biggest improvement in lift happens at higher angles of attack (14° to 18°) because the dome vortex helps generate more lift. However, at lower angles of attack (0° to 6°), the effect of the dome vortex is not as strong, and the lift coefficients have a mixed pattern. The dome vortex also changes the best angle for maximum lift, making



it slightly lower. For example, at an angle of attack of 14° , the dome vortex configuration achieves a lift coefficient of 1.16, which is higher than the lift coefficient of 1.14 for the experimental baseline at the same angle. This means there is an increase of approximately 1.75% in the lift coefficient when using the dome vortex. Similarly, at an angle of attack of 18° , the dome vortex configuration achieves a lift coefficient of 1.27, which is higher than the lift coefficient of 1.15 for the experimental baseline. This corresponds to an increase of approximately 10.43% in the lift coefficient when using the dome vortex.

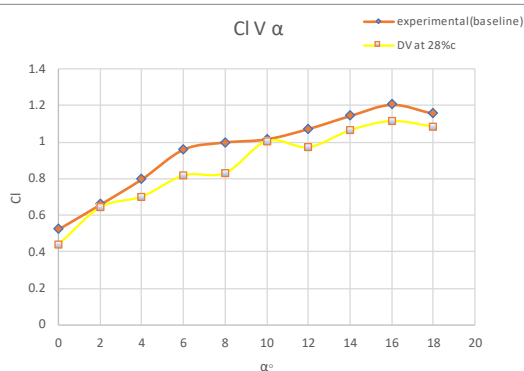


Figure (6): Effect of Dome Vortex at 28% Chord on Lift Coefficient for NACA 4415 Wing at Various Angles of Attack

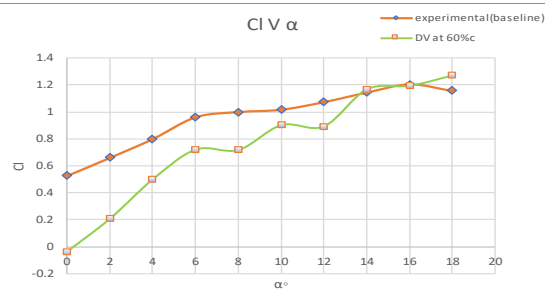


Figure (7): Effect of Dome Vortex at 60% Chord on Lift Coefficient for NACA 4415 Wing at Various Angles of Attack

3. 2. Effect of Converge-Diverge Vortex Location

Figure (8) show, the baseline configuration consistently exhibits higher lift coefficients compared to the converge-diverge vortex at 10% chord across all angles of attack considered. At lower angles, such as 0 degrees and 2 degrees, the difference in lift coefficients between the two configurations is relatively substantial. As the angle of attack increases, the superiority of the baseline becomes more evident. However, at higher angles, such as 16 degrees and 18 degrees, the difference in lift coefficients between the two configurations becomes relatively conservative. Overall, based on the analysis, the experimental baseline configuration demonstrates better lift coefficients than the converge-diverge vortex at 10% chord across the entire range of angles of attack.

Figure (9) illustrates that the baseline configuration consistently exhibits higher lift coefficients compared to the convergent-divergent vortex at 28% chord across various angles of attack. At lower angles, such as 0 degrees and 2 degrees, the

difference in lift coefficients between the two configurations is relatively conservative. The interaction between the dome vortex and the flow plays a significant role in these observations. The dome vortex creates vortices in the flow, which can interact with each other and with the airfoil. This interaction can cause the flow to become more turbulent, resulting in fluctuations in the lift coefficient. However, as the angle of attack increases, the superiority of the baseline configuration becomes more pronounced. At higher angles, such as 12 degrees and 14 degrees, the baseline achieves higher lift coefficients compared to the convergent-divergent vortex at 28% chord.

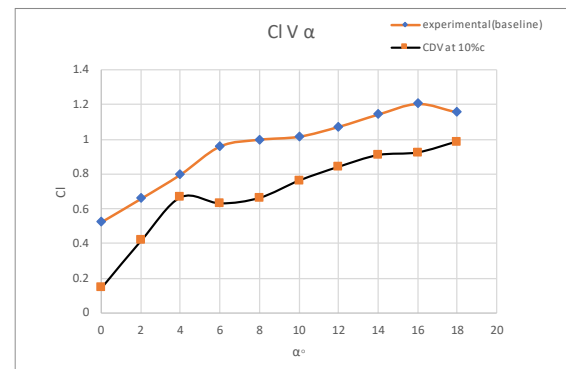


Figure (8): Effect of Converge-Diverge Vortex at 10% Chord on Lift Coefficient for NACA 4415 Wing at Various Angles of Attack

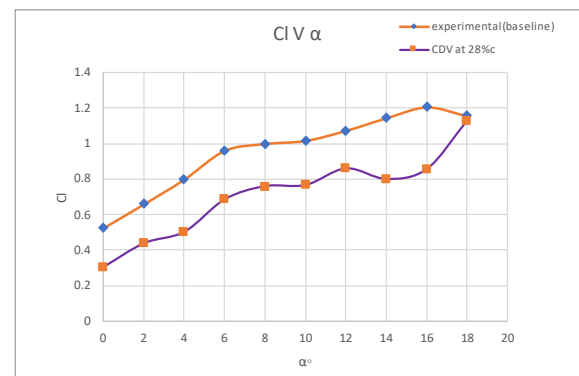


Figure (9): Comparison of Lift Coefficients between Baseline Configuration and Converge-Diverge Vortex at 28% Chord Across Various Angles of Attack

Figure (10) shows that the baseline configuration consistently exhibits higher lift coefficients compared to the convergent-divergent vortex at 60% chord across all angles of attack considered. At lower angles, such as 0 degrees and 2 degrees, the difference in lift coefficients between the two configurations is relatively conservative. However, as the angle of attack increases, the superiority of the baseline becomes more apparent. At higher angles, such as 16 degrees and 18 degrees, the baseline achieves higher lift coefficients compared to the convergent-divergent vortex at 60% chord. The observed fluctuations in the lift curve between angles 4-10 can be attributed to the presence of turbulence induced by the vortex generators. Turbulence can interfere



with the flow, leading to disruptions that contribute to fluctuations in the lift curve. Overall, based on the analysis, the experimental baseline configuration demonstrates better lift coefficients than the convergent-divergent vortex at 60% chord across the entire range of angles of attack.

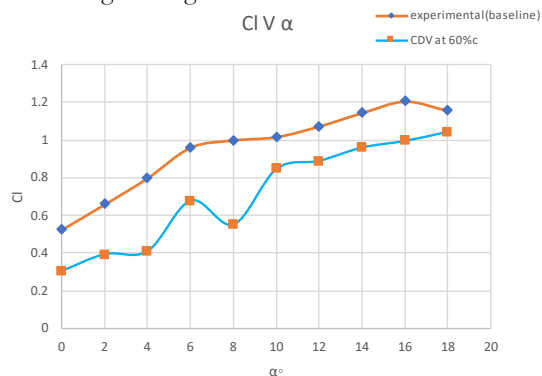


Figure (10): Effect of Converge-Diverge Vortex at 60% Chord on Lift Coefficient for NACA 4415 Wing at Various Angles of Attack

3.3 Compared with a Previous Study

In the previous study [22], the NACA0012 airfoil was employed, whereas the current study focused on the NACA 4415 airfoil. The previous study maintained a consistent position for the vortex generators, located 8% from the leading edge of the airfoil, regardless of the shape (rectangular, triangular, or gothic). On the other hand, the current study examined two types of vortex generators, namely the dome vortex and the converge-diverge vortex, positioned at different chord positions (10%, 28%, and 60% chord) on the NACA 4415 airfoil. Regarding the maximum lift coefficient (C_l), the previous study reported varying values for different vortex generator shapes. The gothic-shaped vortex generator achieved the highest maximum C_l of 1.011 at an angle of attack of 13° . The triangular vortex generator yielded a maximum C_l of 0.9284, while the rectangular vortex generator resulted in a maximum C_l of 0.727. In contrast, the current study discovered a maximum lift coefficient of 1.27 at an angle of attack of 18 degrees for the NACA 4415 airfoil with the dome vortex positioned at 10% chord.

3.4 Drawbacks

Vortex generators provide lift enhancement but come with limitations. They can increase drag by creating turbulence, impacting the lift-to-drag ratio. Alteration of stall characteristics can be problematic, especially in aircraft. Noise generation is a concern, affecting noise-sensitive environments. Installation and maintenance are complex, requiring precise positioning and regular upkeep. Effectiveness varies based on airspeed, angle of attack, and flow conditions. Manufacturing tolerances impact performance, requiring precise dimensions and placement. Surface contamination hinders function, necessitating regular inspection and cleaning. Overcoming these limitations through research and optimization is crucial for maximizing benefits and practical implementation of vortex generators.

4. Conclusions:

1. The lift coefficient curves obtained experimentally and from the Airfoil Tools database demonstrate an increasing trend from 0 to 18 degrees of angle of attack, with deviation beyond 18 degrees indicating an aerodynamic stall. Differences in surface roughness, air density, and temperature contribute to variations between the practical and theoretical curves.
2. At small angles of attack (0 to 8 degrees), the NACA 4415 wing with the dome vortex at 10% chord exhibits lower lift coefficients compared to the baseline. However, at angles beyond 16 degrees, the dome vortex shows higher lift coefficients, reaching a maximum of 1.27 at 18 degrees, surpassing the baseline value of 1.16. This represents a maximum lift coefficient increase of 9.4% compared to the baseline lift coefficient.
3. When using the dome vortex configuration at 60% chord, lift coefficients increase but remain lower than the experimental baseline. The most significant lift improvement occurs at higher angles of attack (14° to 18°), achieving a lift coefficient of 1.16 (representing a 1.75% increase) at 14° and 1.27 (corresponding to a 10.43% increase) at 18° compared to the experimental baseline.
4. Comparisons among different positions of the dome vortex (10% chord, 28% chord, and 60% chord) consistently show that the baseline has higher lift coefficients across all angles of attack. However, the difference in lift coefficients between the baseline and the dome vortex becomes relatively smaller at higher angles, such as 16 and 18 degrees.
5. The dome vortex configuration changes the optimal angle to achieve a higher lift, lowering it slightly. When the dome vortex is positioned at 60% chord and set at a 14-degree angle, the lift coefficient increases to 1.16 compared to the baseline's lift coefficient of 1.14 at the same angle, resulting in a lift increase of approximately 1.75%.
6. Comparisons among different chord positions of the converge-diverge vortex (10% chord, 28% chord, and 60% chord) indicate that the baseline consistently demonstrates better lift coefficients across the entire range of angles of attack. The converge-diverge vortex at 60% chord exhibits the highest lift coefficients among the vortex configurations, particularly at higher angles of attack like 14 and 18 degrees.
7. Despite offering advantages in lift enhancement, vortex generators come with limitations and potential drawbacks. These include increased drag, altered stall characteristics, noise generation, installation and maintenance challenges, limited effectiveness under certain conditions, sensitivity to manufacturing tolerances, and susceptibility to surface contamination.
8. The study recommends that future research investigates the effects of VGs on airfoil shapes other than the NACA 4415, considers different Reynolds numbers and flow conditions, and assesses their performance in aircraft applications.



Additionally, further research could explore the impact of VGs on airfoil-generated noise, heat transfer characteristics, and overall durability.

5. References:

- [1] K. N. Abed, "Flow Separation Control of Backward-Facing Step Airfoil NACA0015 by Blowing Technique," DJES, vol. 12, no. 1, pp. 99-119, 2019. <https://doi.org/10.24237/djes.2019.12111>
- [2] K. N. Abed, "Control of flow separation over NACA 0015 airfoil using synthetic jet actuators: Mechanical," Diyala Journal of Engineering Sciences, pp. 674-685, 2015. <https://djes.info/index.php/djes/article/view/399>
- [3] Hares, et al., "Aerodynamic performances improvement of NACA 4415 profile by passive flow control using vortex generators," Journal of the Serbian Society for Computational Mechanics, vol. 13, no. 1, pp. 17-38, 2019. DOI: 10.24874/jsscm.2019.13.01.02
- [4] O. M. Fouatih, et al., "Design optimization of the aerodynamic passive flow control on NACA 4415 airfoil using vortex generators," European Journal of Mechanics-B/Fluids, vol. 56, pp. 82-96, 2016. doi.org/10.1016/j.euromechflu.2015.11.006
- [5] O. M. Fouatih, B. Imine, and M. Medale, "Numerical/experimental investigations on reducing drag penalty of passive vortex generators on a NACA 4415 airfoil," Wind Energy, vol. 22, no. 7, pp. 1003-1017, 2019. DOI: 10.1002/we.2330.
- [6] N. F. Zulkefli, et al., "Aerodynamic performance of shark skin shape vortex generator," in Proceedings of International Conference of Aerospace and Mechanical Engineering 2019: AeroMech 2019, 20–21 November 2019, Universiti Sains Malaysia, Malaysia, Springer Singapore, 2020. DOI: 10.1007/978-981-15-4756-0_10
- [7] M. T. Jumahadi, et al., "The potential of hybrid micro-vortex generators to control flow separation of NACA 4415 airfoil in subsonic flow," AIP Conference Proceedings, vol. 1930, no. 1, AIP Publishing LLC, 2018. DOI: 10.1063/1.5022924
- [8] X. Li, K. Yang, and X. Wang, "Experimental and numerical analysis of the effect of vortex generator height on vortex characteristics and airfoil aerodynamic performance," Energies, vol. 12, no. 5, p. 959, 2019. DOI: 10.3390/en12050959
- [9] A. Dadamoussa, et al., "Numerical investigation of flow on a Darrieus vertical axis wind turbine Blade with Vortex Generators," International Journal of Fluid Mechanics Research, vol. 47, no. 1, 2020. DOI: 10.1615/InterJFluidMechRes.2020026791
- [10] X.-k. Li, et al., "Analysis of the effect of vortex generator spacing on boundary layer flow separation control," Applied Sciences, vol. 9, no. 24, p. 5495, 2019. DOI: 10.3390/app9245495
- [11] Y. Yan, et al., "CFD analysis for the performance of micro-vortex generator on aerofoil and vertical axis turbine," Journal of Renewable and Sustainable Energy, vol. 11, no. 4, p. 043302, 2019. DOI: 10.1063/1.5110422
- [12] H. Chen, "Numerical investigation of the effects of vortex generators on the Bell A821201 airfoil," Journal of the Brazilian Society of Mechanical Sciences and Engineering, vol. 43, no. 11, p. 516, 2021. DOI: 10.1007/s40430-021-03239-3
- [13] S. Li, et al., "Experimental investigation of a pitch-oscillating wind turbine airfoil with vortex generators," Journal of Renewable and Sustainable Energy, vol. 12, no. 6, p. 063304, 2020. DOI: 10.1063/5.0013300
- [14] Z. Zhao, et al., "Researches on vortex generators applied to wind turbines: A review," Ocean Engineering, vol. 253, p. 111266, 2022. doi.org/10.1016/j.oceaneng.2022.111266
- [15] M. A. Hossain, et al., "Experimental study of aerodynamic characteristics of airfoils using different shaped dimples," The International Journal of Engineering and Science (IJES), vol. 4, no. 1, pp. 13-17, 2015. https://www.ijes.org.pk/papers/Vol4-issue1/Paper_06.pdf
- [16] S. M. A. Aftab and K. A. Ahmad, "NACA 4415 wing modification using tubercles-A numerical analysis," Applied Mechanics and Materials, vol. 629, Trans Tech Publications Ltd, 2014. DOI: 10.4028/www.scientific.net/AMM.629.30
- [17] S. Arunvinthan, et al., "Aerodynamic characteristics of shark scale-based vortex generators upon symmetrical airfoil," Energies, vol. 14, no. 7, p. 1808, 2021. DOI: 10.3390/en14071808
- [18] Z. Laffane, et al., "Numerical investigations of vortex generator effects on the NACA 63-215 wind turbine airfoil," International Journal of Fluid Mechanics Research, vol. 47, no. 6, 2020. DOI: 10.1615/InterJFluidMechRes.2020035335
- [19] E. L. Houghton and P. W. Carpenter, Aerodynamics for engineering students. Butterworth-Heinemann, 2003. <https://www.amazon.com/Aerodynamics-Engineering-Students-L-Houghton/dp/0750651113>
- [20] www.airfoiltools.com/airfoil/details?airfoil=naca4415-il
- [21] Fouatih, Omar Madani, Bachir Imine, and Marc Medale. "Numerical/experimental investigations on reducing drag penalty of passive vortex generators on a NACA 4415 airfoil." Wind Energy vol. 22, no. 7, p. 1003-1017, 2019. DOI: 10.1002/we.2330
- [22] Agarwal, Chaitanya, Ravi Prakash, Vasu Mahajan, Aditya Chhetri, G. Vinaygamurthy, and Awani Bhushan. "Investigation on the Influence of Vortex Generators on Aerofoil." In Conference on Fluid Mechanics and Fluid Power, pp. 263-270. Singapore: Springer Nature Singapore, 2021. DOI: 10.1007/978-981-19-6270-7_46